

Impact of Processing Conditions on Inter-tablet Coating Thickness Variations Measured by Terahertz In-Line Sensing

Hungyen Lin¹, Robert K. May^{1,a}, Michael J. Evans², Shuncong Zhong^{3,b}, Lynn F. Gladden¹,
Yaochun Shen³ and J. Axel Zeitler^{1,*}

¹ Department of Chemical Engineering and Biotechnology, University of Cambridge, Cambridge
CB2 3RA, UK

² TeraView Ltd., St John's Innovation Park, Cambridge, CB4 0DS, UK

³ Department of Electrical Engineering and Electronics, University of Liverpool, Liverpool L69
3GJ, UK

^a present address: TeraView Ltd., St John's Innovation Park, Cambridge, CB4 0WS, UK

^b present address: Department of Naval Architecture, Ocean and Marine Engineering, University
of Strathclyde, G4 0LZ, UK

* Corresponding author: jaz22@cam.ac.uk

Abstract

A novel in-line technique utilising pulsed terahertz radiation for direct measurement of the film coating thickness of individual tablets during the coating process was previously developed and demonstrated on a production scale coater. Here we use this technique to monitor the evolution of tablet film coating thickness and its inter-tablet variability during the coating process under a number of different process conditions that have been purposefully induced in the production scale coating process. The changes that were introduced to the coating process include removing the baffles from the coater, adding uncoated tablets to the running process, halting the drum, blockage of spray guns and changes to the spray rate. The terahertz sensor was able to pick up the resulting changes in average coating thickness in the coating drum and we report the impact of these process changes on the resulting coating quality.

1 Introduction

The process of applying one or more layers of polymer coating onto tablets is almost ubiquitous in pharmaceutical manufacturing in order to simultaneously achieve uniformity of colour, light protection, taste masking and, more recently, to control drug release kinetics and thereby increase the therapeutic efficacy of tablets¹. Tablet coating is typically performed in large batches and the quality of the resulting product is reflected in the intricacies of the tablet mixing dynamics which in turn is dependent on tablet properties (e.g. size and shape), process parameters (e.g. coating pan speed and loading), as well as device specific parameters (e.g. pan diameter, geometry, baffle configuration etc.). In addition to average coating thickness, other metrics that govern the quality of the finished product include intra- and inter-tablet coating uniformity, surface roughness and structural integrity of both the coating and the tablet core.

Various approaches have been employed to gain a better understanding of the complex relationships that exist between the many factors that ultimately determine the coating quality. Recently there has been a significant drive towards systematic process understanding by means of statistical design of experiments as part of the quality-by-design framework that takes account of the manufacturing process from development through to scale-up². While feasible at the development stage, experimental studies made at the production scale are costly and wasteful. An alternative is to undertake rigorous numerical simulation, which has demonstrated tremendous potential for improving the understanding of film coating processes³⁻⁸. Such models can predict both inter-tablet and intra-tablet coating variations, however the accuracy of predictions are subject to the accuracy of the input data, which are often estimates based on assumptions as opposed to the results of measurements made under actual process conditions⁹. In an effort to provide experimental feedback on the coating process, and for possible subsequent process control, different sensor technologies have been introduced to non-destructively measure the tablet coating thickness either in-line or on-line. Examples of such techniques include optical sensing at near-infrared frequencies¹⁰ and Raman spectroscopy¹¹⁻¹³. Comprehensive reviews on the topic have been previously published^{14,15}. Typically, these rapid sensing techniques monitor the spectral attenuation of chemical constituents within the dosage forms directly, from which the average thickness of sampled dosage forms can be inferred using previously created multivariate calibration models. Although these techniques can determine process end-points as well as moisture content that would be important for process control, the calibration models are time-consuming to construct, require ongoing maintenance support and provide prediction performances that are specific to the instrument. Even in cases of the

1
2
3
4
5
6
7 same vendor and model, the transferability of the models is not always seamless and often the
8 models must be reconstructed. Furthermore, the measurements acquired are a time averaged result
9 over the numerous sampled dosage forms and therefore information pertaining to the individual
10 dosage form, such as inter-tablet coating uniformity, is simply unavailable. Other techniques such
11 as optical imaging¹⁶ which, as well as providing tremendous throughput with the use of modern
12 visual imaging systems that reduces the equipment cost barrier, can sample individual tablets and
13 therefore provide information on inter-tablet coating uniformity. However based on the authors'
14 knowledge, optical imaging techniques are currently limited in application to monitoring of
15 spherical dosage forms, largely because of the simplicity involved in determining the coating
16 thickness. Tablets with complex shapes may therefore pose a challenge to thickness calculation.
17 Spectral-domain optical coherence tomography is a recently introduced modality for direct coating
18 thickness measurement of individual dosage forms that boasts high spatial resolution, both laterally
19 and axially^{17,18} therefore making it ideal for measurement of thin coatings. While the technique is
20 promising, especially given its high data acquisition rate, thus yielding inter- and intra-tablet
21 coating uniformity information, the technique is still very much in its infancy thus requiring further
22 research, in particular to assess the maximum thickness coating that can be measured due to the
23 stronger scattering encountered with this technique.
24
25
26
27
28
29
30

31
32 Terahertz pulsed imaging (TPI) was previously demonstrated as a suitable modality to measure the
33 coating thickness of individual pharmaceutical tablets off-line and at-line¹⁹. This measurement
34 technique exploits the fact that the common pharmaceutical excipients, being primarily polymer
35 based, are amorphous and (semi-) transparent to light at terahertz frequencies. Moreover, the
36 coherent and broadband nature of terahertz radiation makes it possible to readily determine the
37 depth at which sub-surface material interfaces occur. By mounting a terahertz sensor externally onto
38 a perforated coating pan such that the tablets inside the rotating coating pan are kept in focus of a
39 continuous train of terahertz pulses, the time lapse between successive reflections from coating
40 interfaces can be measured directly to determine the coating thickness of individual tablets. In order
41 to determine the absolute coating thickness, however, knowledge of the refractive index of the
42 coating material would be required but such information is readily attainable with using
43 terahertz time-domain spectroscopy as outlined previously.²⁰ Compared with the aforementioned
44 measurement techniques, terahertz pulsed technology is quite unique in that it can measure the
45 tablet coating thickness directly and can resolve the thickness of a large number of individual
46 tablets inside the production scale coating pan at any given point in the coating process. Having
47
48
49
50
51
52
53

1
2
3
4
5
6
7 introduced the in-line terahertz pulsed technique previously²⁰, the objective of this study is to
8 further investigate the ability of the technique to monitor changes in the tablet coating thickness
9 distribution inside a production scale film coating unit, in the presence of artificially induced
10 variations in the coating process. Although previous studies have investigated changes in inter-
11 tablet coating uniformity as a result of varying process conditions, those studies were conducted at-
12 line or off-line²¹. In contrast, the present work reports the findings from an in-line investigation
13 conducted in a production scale setting.
14
15
16

17 2 Materials and Methods

18 An in-line terahertz sensor system (TeraView Ltd., Cambridge, UK) was developed and installed on
19 the side of a production scale, side-vented perforated pan tablet coater (Premier 200, Oyster
20 Manesty, Merseyside, UK). To ensure that the generated terahertz pulses were focused onto the
21 surface of tablets inside the coating pan, the sensor was kept at a fixed distance (corresponding to
22 the 7 mm focal length of the sensor optics) from the inner wall of the coating pan. The perforated
23 pan had an overall diameter of 1.3 m, while each circular perforation had a diameter of 3 mm. The
24 patterning of the perforations resulted in a 51% opening on the external surface of the pan. The
25 coating pan was fitted with tubular baffles to facilitate the mixing of the tablet bed. During the
26 coating trial, a polymer film (Acryl-EZE R, Aqueous AcrylicEntericSystem yellow and/or pink,
27 Colorcon Ltd., Dartford, UK) was applied to each batch of tablets. The batch size of uncoated tablet
28 cores was 175 kg. The tablet geometry was bi-convex (10 mm diameter, 370 mg) and consisted of
29 direct compressed lactose monohydrate (Meggler, Wasserburg, Germany). Coating was performed
30 using three spray guns at a spray rate of 300 ml/minute operating at an atomising air pressure of 1.5
31 bar. The coating pan had a rotational speed of 6 rpm. The inlet air flow was set to 2,200 m³/h at a
32 temperature of 52 °C and an absolute water content of 7.6 g/kg. The exhaust temperature was
33 maintained at 38 - 40 °C.
34
35
36
37
38
39
40
41
42

43 The installed terahertz in-line sensor continuously acquired individual terahertz waveforms at a rate
44 of 120 Hz, however not every waveform contains reflections from a tablet surface. Examples of the
45 acquired waveforms are shown in Figure 1. Since the circular openings in the perforated coating
46 pan account for ~~about less than~~ half of the ~~diameter-external surface~~ of the coating pan wall that is
47 presented to the sensor head in each rotation of the coating pan, ~~less than~~ about half of the measured
48 waveforms can contain a reflection that originates from a tablet inside the pan. This number is
49 further reduced since not every aperture will have a tablet directly behind it, nor will all tablets
50
51
52
53

1
2
3
4
5
6
7 behind an aperture be suitably aligned at normal incidence to the terahertz sensor, the optimum
8 orientation needed to obtain a high quality measurement. In order to correctly identify those
9 reflected waveforms that are suitable candidates for subsequent coating thickness calculation, all
10 measured waveforms are automatically processed in real time during data acquisition using the
11 waveform selection algorithm described by the flowchart in Figure 2.
12
13

14
15 Prior to data analysis, signal processing is performed on the raw pulse waveform¹⁹ in order to
16 isolate the sample response from the system response. Generally, the raw pulse waveform shows
17 reflections that arise from each interface or abrupt change in refractive index encountered by the
18 incident terahertz pulse as it propagates into the sample. The relative strength of the reflections
19 indicates the change in physical or chemical composition at the interface. Scattering losses due to
20 e.g. refractive index changes at grain boundaries are typically not significant in pharmaceutical
21 dosage forms due to the absence of structure on length scale of hundreds of micrometres in the
22 coating layers. ~~In particular, The first step in signal processing involves performing a~~ waveform
23 deconvolution with a reference waveform obtained from the ideal reflecting surface of outer
24 metallic mesh wall of the coating pan is performed²⁰ so as to yield time-domain waveforms of a
25 high signal-to-noise ratio that clearly reveal individual reflections from interfaces across which
26 changes in refractive index occur. By applying a set of pre-determined selection criteria to these
27 processed waveforms, only the waveforms that originate from the surface of a coated tablet that is
28 within a range of normal orientation to the terahertz sensor are selected for subsequent coating
29 thickness calculation. Specifically, the position and amplitude of those reflection peaks of interest
30 contained in a given sample waveform must fall within pre-defined limits, as is illustrated in Figure
31 1. A tablet with a single coating contains two reflection peaks of interest: first peak corresponds to a
32 reflection from the air-to-coating interface, and the second peak to a reflection from the coating-to-
33 core interface. The thresholds values are determined from off-line measurements in which reflected
34 waveforms from individual tablets are measured at a series of distances from and angles to the
35 sensor focusing lens so as to identify a suitable peak position and amplitude ranges within which
36 reliable coating thickness can be determined.
37
38
39
40
41
42
43
44
45
46
47

48 The selection criteria are applied to all the processed sample waveform following the flowchart
49 shown in Figure 2. Each must contain a primary reflection peak and the position and amplitude of
50 which lies within the corresponding limits. Examples of waveforms rejected because the primary
51
52

1
2
3
4
5
6
7 reflection peak fails to meet these criteria are shown in Figure 1, where the dashed lines depict the
8 position and amplitude thresholds. If the primary reflection peak satisfies the position and amplitude
9 criteria, analysis is performed with stationary wavelet transform (SWT) to identify the presence of a
10 secondary reflection peak within a realistic pulse delay range (30 to 200 μm). In particular, Haar
11 wavelets are used with four levels of decomposition as it has proven to be a more robust peak
12 finding method in the time-domain²². The amplitude of the secondary pulse within the range (green
13 dashed lines) must then exceed a certain threshold value for coating thickness to be reliably
14 calculated. An example of a waveform that has been rejected from further analysis due to the
15 second reflection peak having an amplitude below the pre-defined amplitude range is also shown. In
16 contrast, bottom right of Figure 2 shows a suitable waveform that has passed all the selection
17 criteria and thus can be used for coating thickness calculation. As coating thickness is directly
18 proportional to the time lapse between consecutive reflection peaks in the time domain and
19 inversely proportional to the refractive index, the coating thickness d is determined as $2d = \Delta t c / n$,
20 where Δt is the time lapse, n is the coating refractive and c is the speed of light in vacuum. In this
21 particular example, the measurement resulted with a coating thickness of 87.6 μm for a coating
22 refractive index of 1.55.
23
24
25
26
27
28
29
30

31 The particular values assigned to the reflection peak position and amplitude limits must be carefully
32 chosen so as to maximise the number of measured tablets, while simultaneously ensuring that only
33 high quality waveforms are accepted so as to omit low confidence coating thickness readings. Using
34 the most stringent values for the selection criteria to ensure acceptance of high quality waveforms
35 only, a tablet hit rate of 8,200 (~0.3% of all measured waveforms) over 6 hours of tablet coating
36 was achieved, which corresponds to a 'hit rate' of over 20 individual tablets per minute. For a single
37 coating run with steadily increasing coating thickness, a value of $R^2 = 0.91$ and a root mean squared
38 error (RMSE) = 5.8 μm were determined for this set of processing parameters when correlated with
39 off-line terahertz thickness measurements made on coated tablets removed at regular intervals
40 during the coating process. In order to optimise the threshold values used by the selection criteria,
41 while taking account of possible experimental uncertainties and the non-concentric nature of the
42 coating pan, a systematic study was conducted to optimise the hit rate. Specifically, we generated a
43 set of possible values for the selection parameters and then tested them when analysing the data
44 from a single tablet coating run. The optimal values for the various selection thresholds were
45 determined by using numerical optimisation to maximise the number of measured tablets whilst
46
47
48
49
50
51
52

1
2
3
4
5
6
7 simultaneously maximising the agreement between on-line and off-line thickness measurements (in
8 terms of R^2 and RMSE values). To speed up computation, different selection criteria were applied
9 to the acquired waveforms in parallel on a cluster of four workstations under the Matlab Parallel
10 Computing Toolbox environment (Matlab R2012, The MathWorks Inc., Natick, MA, USA).
11
12

13
14 The optimal selection criteria that were identified from this run were subsequently applied to the
15 experimental measurements acquired from a number of coating runs where process variations were
16 artificially induced into the coating process. These variations include the removal and insertion of
17 mixing baffles, the addition of uncoated tablet cores into the pan at a later process time point, and
18 altering the coating spray rates during the coating process.
19
20

21 **3 Results and discussions**

22
23 By using the optimal selection criteria, the number of total tablet hits can be increased from 8,200 to
24 16,660, resulting in a value of $R^2 = 0.8$ and $RMSE = 10 \mu\text{m}$, a notable decrease in R^2 value that
25 produces significant improvement in the hit rate. Despite the reduction in R^2 value, data quality is
26 generally not compromised, however we note the introduction of artefacts (thickness $\sim 150 \mu\text{m}$)
27 present in the coating thickness distributions. The strongest influence on the hit rate was found to be
28 the selection criterion for the primary reflection (air to coat interface). This can be explained by the
29 fact that the coating pan is not perfectly concentric thus causing subtle and systematic changes to
30 the position of the measured terahertz waveform in every rotation of the pan. As a result of relaxing
31 the selection criteria for the location of the first reflection peak to account for the concentricity
32 imperfections of the coating pan, additional reflections are considered for thickness calculation. The
33 study to determine the optimal selection criteria took approximately one week with 2 workers on
34 the cluster. This time could be significantly reduced by using a factorial design with a reduced
35 number of combinations and by performing the parallelisation of the code that can be executed on
36 the GPU rather than the CPU.
37
38
39
40
41
42
43

44
45 By using the optimal selection criteria on the acquired waveforms it is possible to maximise the
46 amount of tablet coating thickness data that can be extracted from the process to analyse the effect
47 of process changes on the inter-tablet coating thickness distribution. Figure 3 shows distributions of
48 tablet coating thickness from data acquired over 20 minute windows (using histogram bin widths of
49 $5 \mu\text{m}$) for the previously published coating run²⁰. During the first 60 to 80 min of the process, the
50 coating thickness is below the minimum resolvable thickness²⁰. Assuming a normal distribution for
51
52
53

1
2
3
4
5
6
7 coating thickness distribution in each time window, the mean and variance of each coating
8 thickness distribution was estimated by fitting, in a least-squares sense, a Gaussian profile to each
9 histogram. Since all captured reflections may not originate from tablet surface or the centre band,
10 the data may be better described with alternative distributions such as F, Chi or Rayleigh
11 distributions. Further work will aim to better discriminate the reflections from the tablet surface and
12 from the centre band. In general, the underlying distribution would be probabilistically dependent
13 on additional parameters not limited to tablet geometry, including the loading level of the coating
14 pan and the rotational speed. Nevertheless, Figure 4 shows the curve-fitted mean and the coefficient
15 of variation (CoV) or the inter-tablet coating thicknesses variability with respect to coating time.
16 Note that the CoV is determined using the relative standard deviation (in %) as opposed to the
17 absolute standard deviation in μm . As numerous studies have been carried out in literature on
18 predicting CoV using discrete element method (DEM)^{3,4,23} based on residence time distributions,
19 CoV of the present experimental study has therefore been plotted on a log-log scale for direct
20 comparison and hence consolidation. Specifically, the decreasing CoV is fitted with a straight line
21 with a slope of -0.57, slightly higher in magnitude than the reported value of -0.5, which was found
22 to describe the coating behaviour of tablets on a lab scale coater³. Despite the agreement, the values
23 of the CoV are approximately an order of magnitude greater than those of the CoV measured in
24 an off-line setting²¹. The high variability observed in our experiments nevertheless is
25 consistent in agreement with the findings reported in the previously published coating run²⁰
26 especially and can be explained by the fact considering that two orders of magnitude more tablets
27 were sampled in the in-line analysis than in compared to the off-line analysis.

3.1 Effect of Removing Coater Baffles

38
39 Figure 5 shows the tablet coating thickness distributions over 20 minute windows for a coating run
40 in which the mixing baffles were removed after 200 minutes of coating. Figure 6 shows the
41 corresponding curve-fitted mean and the CoV as a function of coating time. After 80 minutes of
42 coating time we observe a monotonic increase in tablet coating thickness. The inter-tablet coating
43 thickness variability also decreases monotonically until just after 200 minutes of process time
44 (about 220±5 minutes), beyond which the trend remains relatively constant, which coincides
45 with From the time the removal of the mixing baffles are removed the CoV does not decrease further
46 but remains constant at around 25%. It is interesting to note that the mean coating thickness appears
47 to be unaffected by the removal of the baffles. The decrease in CoV up to the point where the
48
49
50
51
52

1
2
3
4
5
6
7 mixing baffles have been removed is fitted to a straight line with a slope -0.61, similar to the value
8 of -0.57 obtained for the previous coating run in Figure 4²⁰. Even though the slope is slightly higher
9 in magnitude than the previously reported³ value of -0.5, considering the many discrepancies that
10 exist between the parameters used in the DEM simulation and the actual experimental conditions
11 this value is in surprisingly close agreement. The main differences lie in the scale of the present
12 operating conditions compared to those of the simulation: the coater diameter (1.3 m compared to
13 0.62 m), tablet load (473,000 tablets compared to 22,500) and the number of spray nozzles (3
14 compared to 1). All of these factors will affect the tablet residence time within the spray zone. It
15 should also be highlighted that measurement uncertainties were inadvertently introduced by
16 relaxing the selection criteria to overcome the concentricity imperfections of the coating pan. The
17 new selection criteria nonetheless produced a relatively steady hit rate throughout the process, as
18 shown in Figure 6, that was necessary for the process investigation.
19
20
21
22
23
24

25 **3.2 Addition of Uncoated Cores During the Coating Process**

26 In another coating run, 87.5 kg of uncoated tablet cores (Tablets B) were added to the coating pan at
27 approximately 140 minutes into the coating process of an initial batch of the same size (Tablets A).
28 Coating was applied to the combined batches for a further 80 minutes for a total coating time of 220
29 minutes. Figure 7 shows that the resulting changes to the coating thickness distributions. The
30 emergence of two distinct coating thickness distributions representing the initial batch 'Tablets A'
31 and the additional batch 'Tablets B' is clearly visible after 140 minutes. At the same time, there is a
32 clear shift in the original single coating distribution implying continued increasing thickness in the
33 coating of Tablets A. The width and CoV of the two separate Gaussian approximated distributions
34 of Tablets A and Tablets B are plotted in Figure 8. The plot of CoV over the entire coating trial
35 shows that that coating thickness variability increases sharply as a whole following the insertion of
36 Tablets B until 160 minutes of the process, but gradually reduces thereafter, which is in good
37 qualitative agreement with simulations³. During previous coating trials conducted under the same
38 process conditions, the minimum resolvable coating thickness of 30 to 40 μm was detected after
39 approximately 80 minutes of coating time. Since this corresponds to the total duration that Tablets
40 B were coated for, we should not expect changes to the coating on those tablets. The coating
41 thickness distribution during the first 80 minutes interval, nevertheless appears to take the form of
42 Gaussian distribution centred around 40 to 50 μm . By introducing uncoated cores into an already
43 coated batch of the same size, we speculate that it may take twice as long to reach the minimum
44
45
46
47
48
49
50
51
52

1
2
3
4
5
6
7 resolve coating thickness. With an increase in the total tablet population, the number of tablet hits
8 did not increase during the interval 140 - 160 minutes. Beyond this point, however, the number of
9 tablet measurements remained relatively steady with increasing coating time. It should be noted that
10 since the coating thickness distributions are relatively broad, there is an overlap between the
11 respective thickness distributions and therefore the tablet hits for Tablet A and B are approximated
12 from the area underneath their respective distributions respectively, while the figure for the total
13 tablet hits is representative of the total number of measurements acquired. With reference to Figure
14 8, the sharp decline in the hit rate of Tablet A coincides timely with the insertion of the tablet cores
15 and hence the sharp increase in the hits rate of Tablet B. Following on, the hit rate for Tablet B
16 nevertheless remains relatively constant. The subsequent slow reduction in hit rate of Tablet A can
17 be attributed to the particular selection criteria that were chosen for the detection of tablets with
18 thinner coatings. Specifically, the thresholds used in the analysis were defined for thinly coated
19 tablets only, so as the coating grows thicker, the position and amplitude of the reflection peaks fall
20 outside the detection thresholds for such tablets. An obvious way to alleviate this deficiency would
21 be to define the thresholds on the basis of a worst case scenario, i.e. thickest achievable coats.
22 However by doing so, the accuracy of the measurements may become questionable as more coating
23 reflections, not only just the normal reflections may be permitted for thickness measurement.
24 Clearly more work is needed in this regard to dynamically adjust the thresholds or define more than
25 one set of selection criteria for each thickness population in order to capture high quality reflections
26 that would unveil more precise insights on the inter-tablet coating uniformities. However, the
27 coating scenario tested in this run is completely artificial and extreme. During normal processing
28 such vast variation in coating thickness is highly unlikely.

3.3 Further Deliberate Modifications of the Process Conditions

39
40
41 The ability of terahertz to detect and report changes in coating thickness due to changes in process
42 conditions was further tested through additional coating trials conducted under non-standard, yet
43 commonly encountered undesirable process conditions with changes that included halting the
44 coating pan, intermittent blockage of the spray guns and deliberate variation of spray rates. The
45 measured thickness distributions after 80 minutes of coating are shown in Figure 9 (note the
46 differences in relative hit rates in each 20 minute interval). The best-fit Gaussian mean and variance
47 of the thickness distribution are shown as a function of process time in Figure 10. During the 80 to
48 206 minutes period (region I in Figure 10), pan rotation was repeatedly halted for short periods and
49
50
51
52

1
2
3
4
5
6
7 spray was stopped for the intermittent cleaning of the spray guns (80-114 minutes). In the period
8 from 114 to 206 minutes the pan was set to jog with all spray operation stopped. The lack of pan
9 rotation resulted in a localised and repeated measurement of a small sub-population of tablets
10 leading to a relatively low and constant number of hits. As such, the thickness values derived during
11 this period have a low level of confidence. From 206 to 238 minutes (region II), pan rotation and
12 spray was restarted. A different coating colour was used subsequently (change from Acry-EZE pink
13 to Acry-EZE white). As demonstrated previously, colour changes has little to no effect in the TPI
14 coating thickness measurement as the optical properties at terahertz frequencies are not significantly
15 affected by this change in pigment or lake as long as the overall bulk polymer of the coating
16 formulation is unaffected²⁰. Without any further perturbation to the coating process, an increased
17 number of measurements were acquired (reflected by the monotonic rise of hits), and the measured
18 coating thickness increased slightly (~5 µm). The level of inter-tablet coating uniformity-variability
19 also increases monotonically in this period. During the 238 to 290 minutes period (region III) the
20 spray rate was reduced due to intermittent blockages in the spraying guns, the effect of which can
21 be observed in the slight decline of the rate of increase in the mean coating thickness. This trend
22 also appears to be replicated in the inter-tablet coating thickness variability as well. Finally, from
23 300 minutes onwards (region IV) the mean thicknesses and variability plateaus, which coincides
24 with the turning off of the spray guns in an effort to increase the exhaust temperature for the
25 conclusion of the process at 330 minutes.
26
27
28
29
30
31
32
33

34 **4 Conclusion**

35
36 In this study, we have outlined a systematic strategy to optimise the waveform selection algorithm
37 for the coating thickness analysis using a TPI in-line sensor in order to cater for the non-
38 concentricity of the coating pan. We have also demonstrated for the first time the use of an in-line
39 terahertz sensor to study the effect of changes in the inter-tablet coating thickness distribution as the
40 result of process variations during the tablet coating process. Our experimental results show that the
41 removal of mixing baffles during the coating process will produce tablets with a higher level of
42 coating thickness variation, evidently due to poorer mixing of tablets. Adding a batch of uncoated
43 tablets during the coating operation resulted in the clear observation of two distinct thickness
44 populations and clearly demonstrated both the sensitivity and the robustness of the TPI technique
45 for pharmaceutical coating process sensing. The effect of other process changes such as reducing
46 the spray rate and halting the coating pan during the coating process were also demonstrated, and
47 resulted in a clear measurement response of the terahertz in-line sensor. With the increased
48
49
50
51
52
53

1
2
3
4
5
6
7 affordability of computational power, together with numerical modelling such as DEM, terahertz in-
8 line sensor technology can play a vital role to unveil new insights into the film coating processes of
9 pharmaceutical tablets as it is currently the only technology demonstrated on a production-scale
10 setting that is capable of resolving inter-tablet coating variations in situ and in-line. Such an
11 understanding is critical to the successful development of high quality advanced drug delivery
12 systems such as active coatings and sustained release coatings. At the same time, future work will
13 also aim to overcome the minimum resolvable coating thickness limitation of 30 to 40 μm by
14 integrating optical coherence tomography with terahertz in-line sensing to further investigate the
15 pharmaceutical film coating process.
16
17
18
19

20 Acknowledgements

21
22 This work was conducted with financial support from the UK Technology Strategy Board
23 (AB293H). H.L. And J.A.Z. would like to acknowledge the Engineering and Physical Sciences
24 Research Council (EP/L019922/1) and the Newton Trust Cambridge for research funding. J.A.Z.
25 would like to thank Gonville & Caius College, Cambridge for a research fellowship. The authors
26 acknowledge Colorcon Ltd. and Meggle AG for providing the excipients used in this study, Provel
27 Ltd. (Bolton, UK) for the kind loan of the mixing equipment to disperse the coating polymer and
28 Staffan Folestad (AstraZeneca) for useful discussions.
29
30
31
32
33
34
35
36
37
38
39
40
41
42
43
44
45
46
47
48
49
50
51
52
53
54
55
56
57
58
59
60

References

1. McGinity JW, Felton LA. 2008. Aqueous polymeric coatings for pharmaceutical dosage forms. 3rd ed. ed., London: Informa Healthcare.
2. Dubey A, Boukouvala F, Keyvan G, Hsia R, Saranteas K, Brone D, Misra T, Ierapetritou MG, Muzzio FJ 2012. Improvement of tablet coating uniformity using a quality by design approach. *AAPS PharmSciTech* 13(1):231-246.
3. Kalbag A, Wassgren C 2009. Inter-tablet coating variability: Tablet residence time variability. *Chem Engin Sci* 64(11):2705-2717.
4. Ketterhagen WR 2011. Modeling the motion and orientation of various pharmaceutical tablet shapes in a film coating pan using DEM. *Int J Pharm* 409(1-2):137-149.
5. Suzzi D, Radl S, Khinast JG 2010. Local analysis of the tablet coating process: Impact of operation conditions on film quality. *Chem Eng Sci* 65(21):5699-5715.
6. Suzzi D, Toschkoff G, Radl S, Machold D, Fraser SD, Glasser BJ, Khinast JG 2012. DEM simulation of continuous tablet coating: Effects of tablet shape and fill level on inter-tablet coating variability. *Chem Eng Sci* 69(1):107-121.
7. Turton R 2010. The application of modeling techniques to film-coating processes. *Drug Dev Ind Pharm* 36(2):143-151.
8. Werner SRL, Jones JR, Paterson AHJ, Archer RH, Pearce DL 2007. Air-suspension particle coating in the food industry: Part I — state of the art. *Powder Tech* 171(1):25-33.
9. Just S, Toschkoff G, Funke A, Djuric D, Scharrer G, Khinast J, Knop K, Kleinebudde P 2013. Experimental analysis of tablet properties for discrete element modeling of an active coating process. *AAPS PharmSciTech* 14(1):402-411.
10. Kirsch JD, Drennen JK 1996. Near-infrared spectroscopic monitoring of the film coating process. *Pharm Res* 13(2):234-237.
11. El Hagrasy A, Chang S-Y, Desai D, Kiang S 2006. Raman spectroscopy for the determination of coating uniformity of tablets: assessment of product quality and coating pan mixing efficiency during scale-up. *J Pharm Innov* 1(1):37-42.
12. Muller J, Brock D, Knop K, Zeitler JA, Kleinebudde P 2012. Prediction of dissolution time and coating thickness of sustained release formulations using Raman spectroscopy and terahertz pulsed imaging. *Eur J Pharm Biopharm* 80(3):690-697.
13. Romero-Torres S, Pérez-Ramos JD, Morris KR, Grant ER 2005. Raman spectroscopic measurement of tablet-to-tablet coating variability. *J Pharm Biomed Anal* 38(2):270-274.
14. De Beer T, Burggraef A, Fonteyne M, Saerens L, Remon JP, Vervaet C 2011. Near infrared and Raman spectroscopy for the in-process monitoring of pharmaceutical production processes. *Int J Pharm* 417(1-2):32-47.
15. Knop K, Kleinebudde P 2013. PAT-tools for process control in pharmaceutical film coating applications. *Int J Pharm* 457(2):527-536.
16. Oman Kadunc N, Sibanc R, Dreu R, Likar B, Tomazevic D 2014. In-line monitoring of pellet coating thickness growth by means of visual imaging. *Int J Pharm* 470(1-2):8-14.
17. Markl D, Zettl M, Hanneschläger G, Sacher S, Leitner M, Buchsbaum A, Khinast JG 2014. Calibration-free in-line monitoring of pellet coating processes via optical coherence tomography. *Chem Eng Sci* 125(0):200-208.
18. Markl D, Hanneschläger G, Sacher S, Leitner M, Khinast JG 2014. Optical coherence tomography as a novel tool for in-line monitoring of a pharmaceutical film-coating process. *Eur J Pharm Sci* 55(0):58-67.

19. Zeitler JA, Shen Y, Baker C, Taday PF, Pepper M, Rades T 2007. Analysis of coating structures and interfaces in solid oral dosage forms by three dimensional terahertz pulsed imaging. *J Pharm Sci* 96(2):330-340.
20. May RK, Evans MJ, Zhong S, Warr I, Gladden LF, Shen Y, Zeitler JA 2011. Terahertz in-line sensor for direct coating thickness measurement of individual tablets during film coating in real-time. *J Pharm Sci* 100(4):1535-1544.
21. Brock D, Zeitler JA, Funke A, Knop K, Kleinebudde P 2014. Evaluation of critical process parameters for inter-tablet coating uniformity of active-coated GITS using Terahertz Pulsed Imaging. *Eur J Pharm Biopharm* 88(2):434-442.
22. Zhong S, Shen YC, Evans M, Zeitler JA, May RK, Gladden LF, Byers C. Infrared, Millimeter, and Terahertz Waves, 2009 IRMMW-THz 2009 34th International Conference on, 21-25 Sept. 2009, pp 1-2.
23. Toschkoff G, Just S, Funke A, Djuric D, Knop K, Kleinebudde P, Scharrer G, Khinast JG 2013. Spray models for discrete element simulations of particle coating processes. *Chem Eng Sci* 101(0):603-614.

Figures

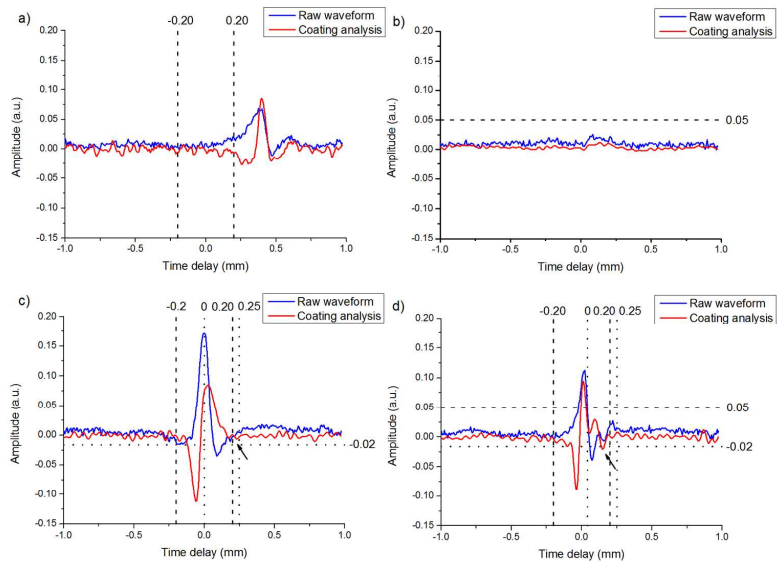
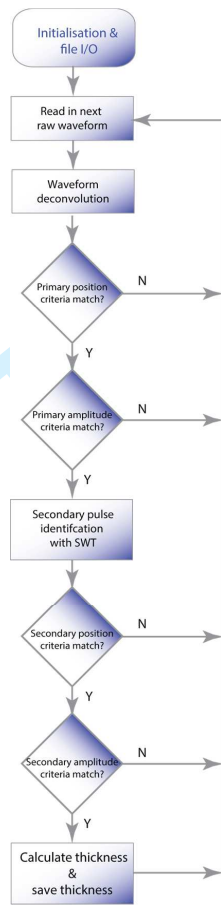


Figure 1 - Examples of three rejected waveforms and one accepted waveform (d). An example of the waveform for failing outside the primary pulse position range (a), the primary pulse amplitude range (b) and the secondary pulse amplitude range (c), and an accepted waveform that satisfies all these criteria (d) with an arrow pointing the secondary peak.



Formatted: Keep with next

Figure 2 - Activity diagram of the data processing algorithm to systematically identify high quality waveforms for use in coating thickness determination from in-line data acquired and processed in real time.

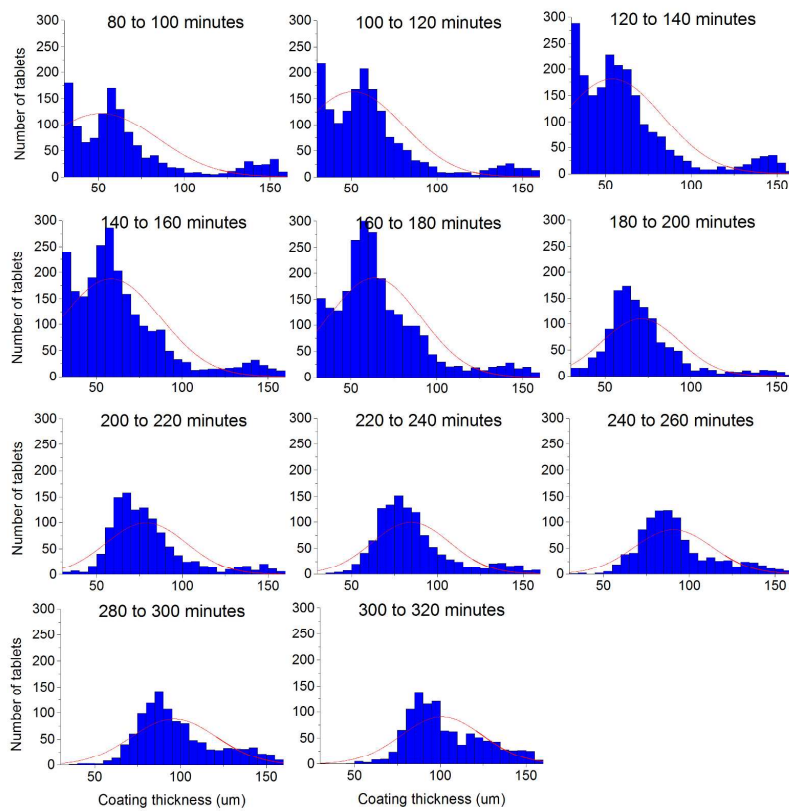
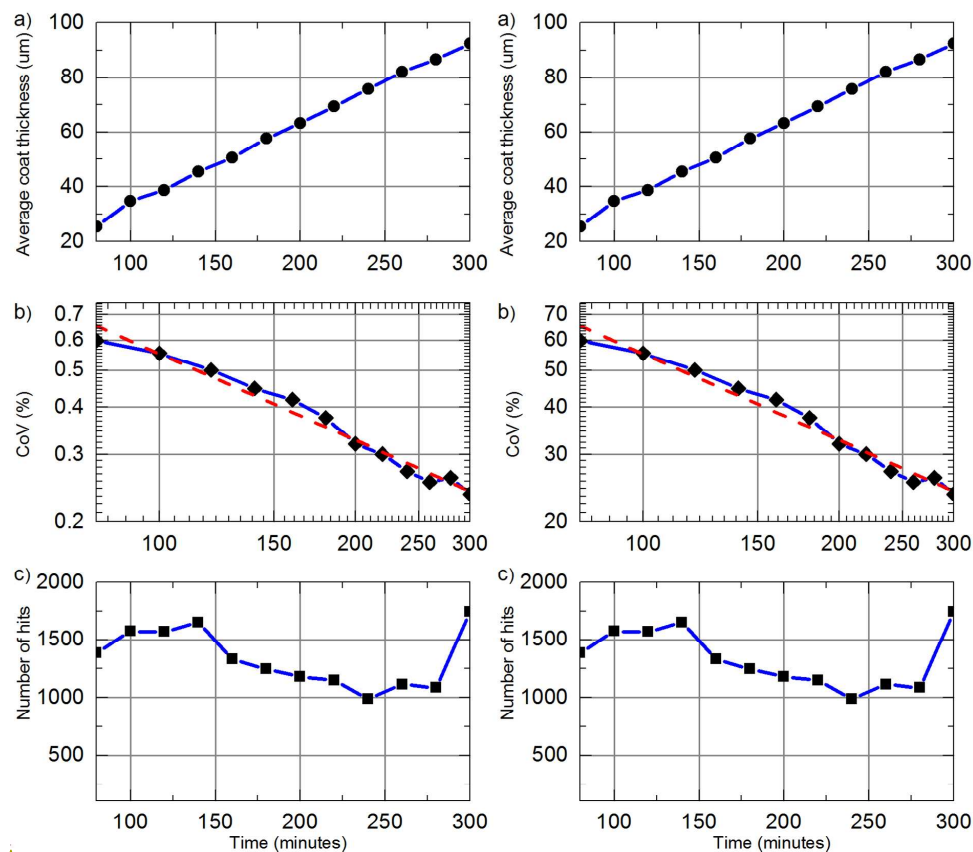


Figure 332 - Histogram of tablet coating thicknesses inside the coating pan from 80 to 320 minutes for the previously published coating run²⁰. The large thickness values (> 150 μm) acquired does not represent a reliable measurement and is an artefact due to relaxed acceptance criteria.



Formatted: Font: 12 pt, Not Bold

Figure 443 - Curve-fitted mean (a) and inter-tablet variability (log-log scale) (b), as well as the number of coated tablet thickness measurements (c) during for a previously published coating run²⁰. The linear decrease in the inter-tablet variability is curve-fitted with a red dashed line to extract the rate of decrease.

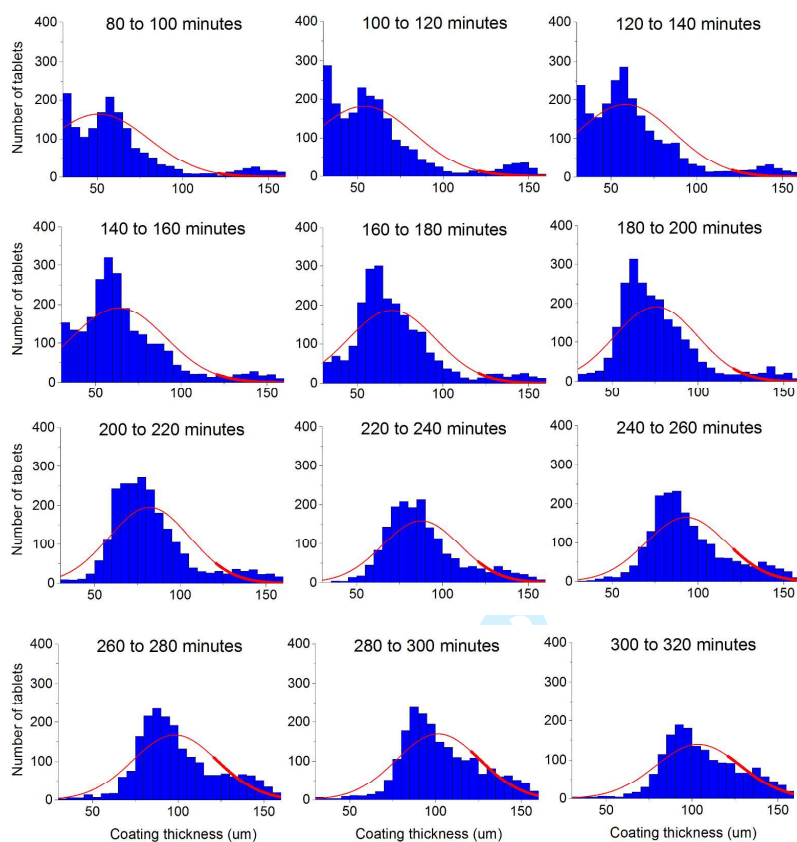
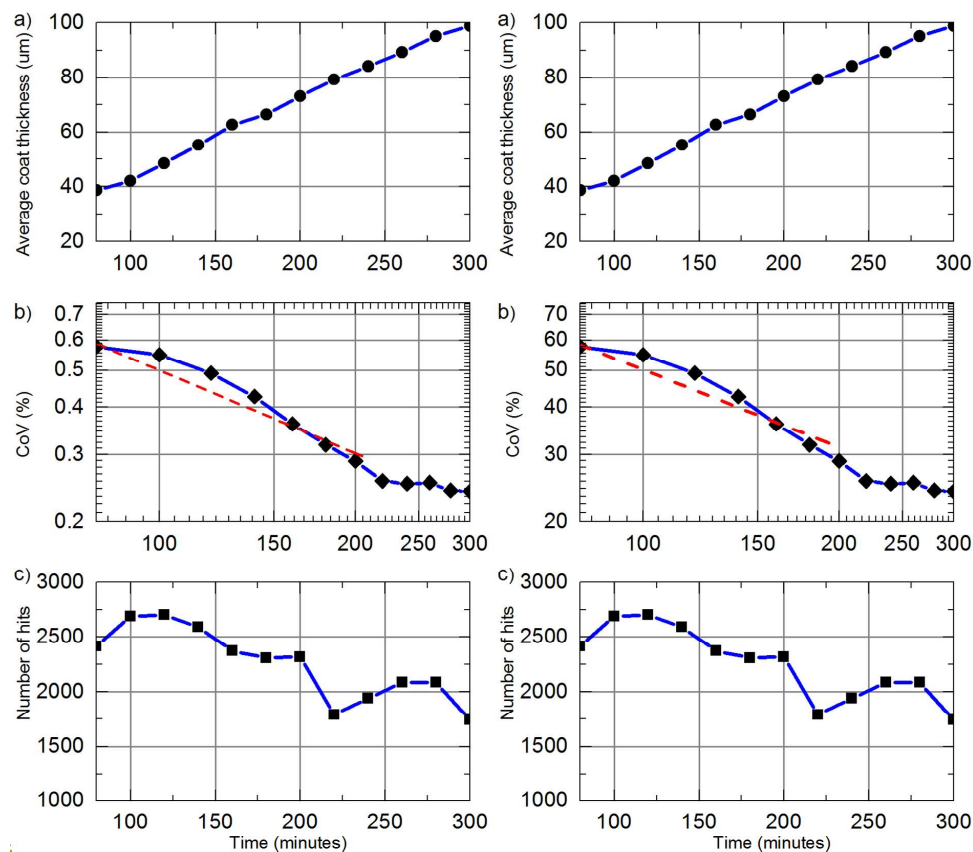


Figure 554 - Histogram of tablet coating thicknesses inside the coating pan from 80 to 320 minutes. The large thickness values ($> 150 \mu\text{m}$) acquired do not represent reliable measurements and are artefacts due to relaxed acceptance criteria.



Formatted: Font: 12 pt, Not Bold

Figure 665 - Curve-fitted mean (a), inter-tablet variability (log-log scale) (b) and number of tablet coating thickness (c) during a coating run where the baffles were removed after 200 min process time. Lines are plotted to guide the eye. The linear decrease in the inter-tablet variability is curve-fitted with a red dashed line to extract the rate of decrease.

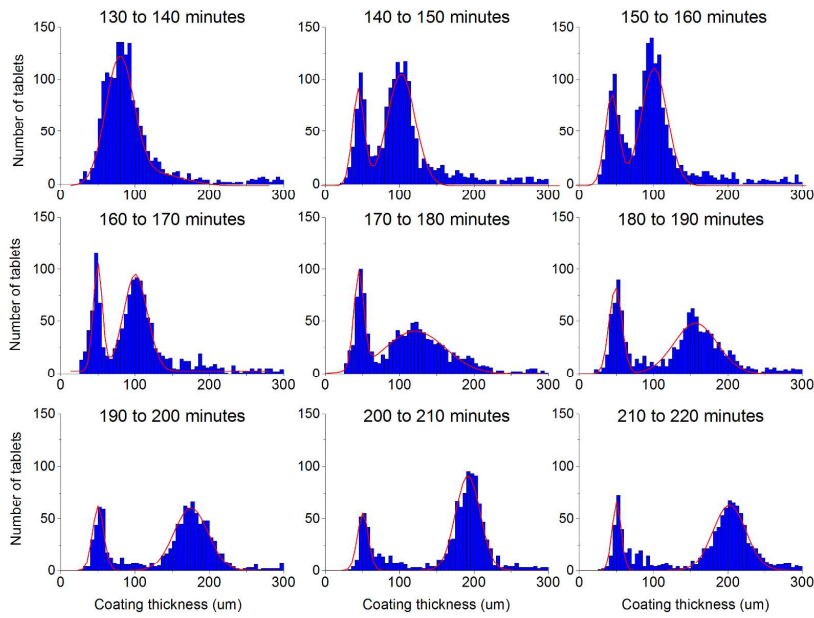
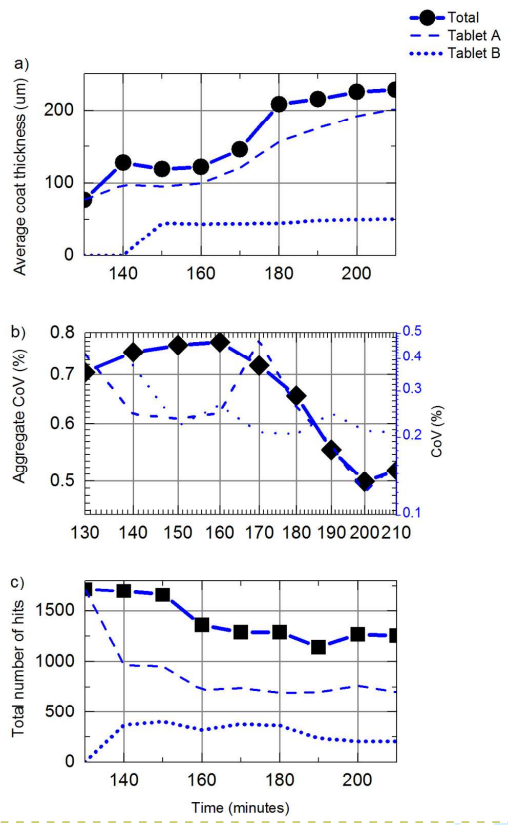


Figure 776 - Histogram of tablet coating thicknesses from 130 to 220 minutes with uncoated tablets introduced close to 140 minutes of the coating process.

1
2
3
4
5
6
7
8
9
10
11
12
13
14
15
16
17
18
19
20
21
22
23
24
25
26
27
28
29
30
31
32
33
34
35
36
37
38
39
40
41
42
43
44
45
46
47
48
49
50
51
52
53
54
55
56
57
58
59
60



Formatted: Font: 12 pt, Not Bold

Review

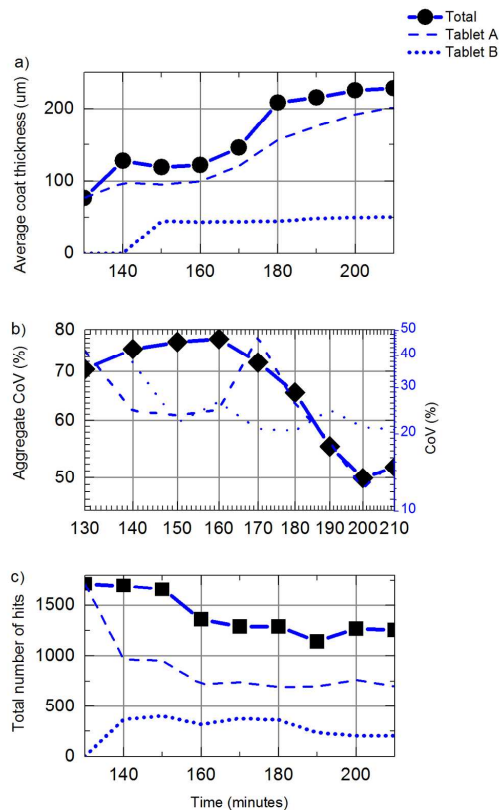


Figure 887 - Curve-fitted mean (a), inter-tablet variability based on the width of the Gaussian approximated distribution (log-log scale) (b) and the number of hits (c) of the total population, Tablet A and Tablet B where uncoated tablets (Tablet B) were introduced close to 140 minutes of the coating process.

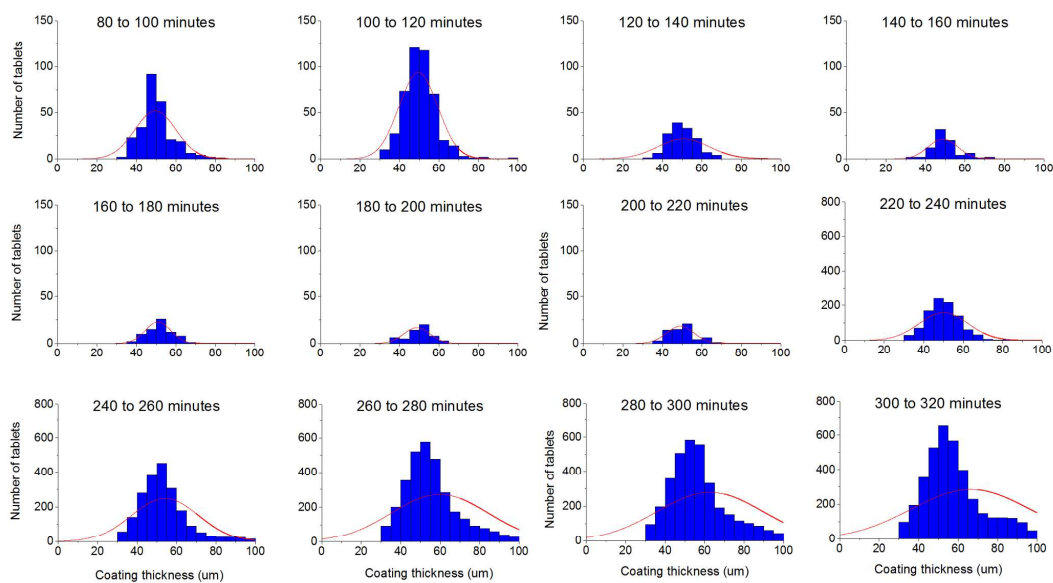


Figure 998 - Histogram of tablet coating thicknesses inside the coating pan from 80 to 320 minutes of the coating process where during the process, there were intermittent disruptions to the spray rate.

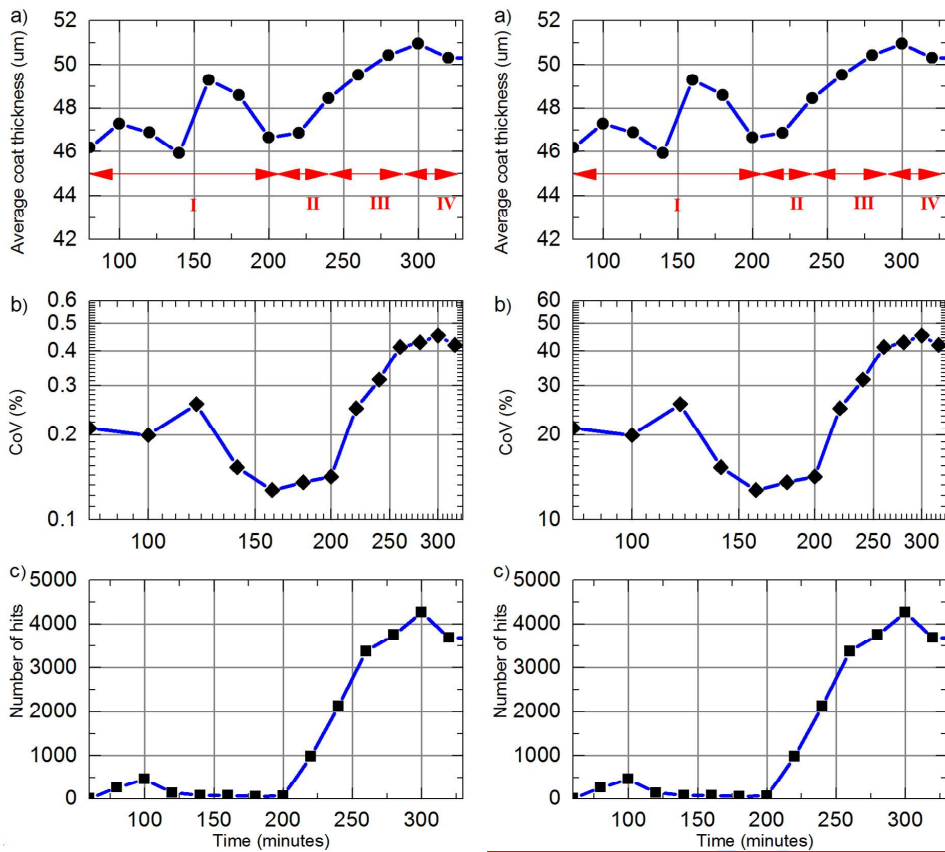


Figure 10109 - Curve-fitted mean (a), inter-tablet variability (log-log scale) (b) and number tablet coating thicknesses (c) under various process perturbations at different time periods such as halting pan rotation due to spray gun blockage (I), restart coating (II), reducing spray rate (III) and stop spraying (IV).